Solvent-Induced Organization of Amorphous Isotactic Polystyrene

Said El Hasri,[†] Biswajit Ray,[‡] Annette Thierry, and Jean-Michel Guenet*

Institut Charles Sadron, CNRS UPR 22, 6, rue Boussingault, F-67083 Strasbourg Cedex, France

Received February 12, 2004; Revised Manuscript Received March 23, 2004

ABSTRACT: The thermodynamic behavior, the morphology, and the molecular structure of systems prepared from exposure to liquid solvent (*cis*- and *trans*-decalin) of solid isotactic polystyrene samples at different temperatures (4−40 °C) are reported. No significant differences are detected when comparison is made with solution-cast samples prepared by a rapid cooling at the same temperatures. This shows again that the formation of these systems is independent of the path followed: varying concentration at constant temperature (solvent-exposed) or varying temperature at constant concentration (solution cast) produces the same effects.

Introduction

Crystals or gels from stereoregular polymers can be produced for investigation purposes through the cooling of homogeneous solutions[1−3] (solution-cast process) or through exposure of a solid sample to solvent liquid or vapors[4−8] (solvent-induced process). The latter process is of special interest as it can be achieved at or close to room temperature as opposed to heating to high temperature required for preparing homogeneous solutions. Also, it gives an insight into what has been termed "physical corrosion" of solid crystalline polymers.[9] Indeed, stereoregular polymers tend to form polymer−solvent compounds,[4−8,10] the growth of which renders significantly rougher the initially smooth surface of the solid polymer, a phenomenon which is reminiscent of chemical corrosion effects although being due to a purely physical effect. As has been shown, the state of the resulting surface depends strongly upon the solvent type as well as upon the exposure temperature.[4−9] Recent thermodynamic investigations of solvent-induced samples from syndiotactic polystyrene have also highlighted the invariance of the melting properties with respect to the path followed to reach a *T*,*C* coordinate of the temperature−concentration phase diagram.[8] Whether the system is obtained at constant concentration from a homogeneous solution or at constant temperature from a solid sample exposed to solvent makes no significant difference. This outcome further suggests that Gibbs phase rules can be applied to these supposedly out-of-equilibrium systems that eventually behave like systems at equilibrium.

In this paper further investigation of the solvent-induced crystallization process has been carried out by using isotactic polystyrene (iPS). The stereoisomers of decalin, namely cis- and *trans*-decalin, have been selected on account of the large number of papers devoted to these systems but also because of the wealth of differing phases produced in these solvents.[11] In particular, the numerous experimental evidence for polymer−solvent compound formation[10−15] makes it an interesting system for comparison with results obtained with syndiotactic polystyrene systems. As will be detailed hereafter, the same phases as those grown from solution-cast samples are obtained with solvent-exposed samples within the same temperature and polymer concentration ranges.

Experimental Section

Materials. The isotactic polystyrene sample was synthesized following the method devised by Natta.[16] ^{1}H NMR characterization showed that the content of isotactic triads was over 99%.[10,11] The different moments of the molecular weight distribution were determined by GPC in THF at room temperature with silica gel columns calibrated by means of the universal calibration method.[17,18] The following values were obtained: $M_w = 1.0 \times 10^5$ with $M_w/M_n = 4.4$.[10,11] *cis*-Decalin and *trans*-decalin were purchased from Aldrich and used without further purification.

Sample Preparation. The solvent-induced bulk samples were obtained from bubble-free disk-shaped pieces (20 mm diameter, 0.1 mm thickness) molded under vacuum at 250 °C, quenched into ice−water, properly dried, and exposed to liquid solvents at different temperatures.

Exposure times were approximately 1 month while keeping the samples in thermally regulated cells (±1 °C). A few samples were investigated after 6 months and 1 year exposure to liquid solvent but displayed no detectable differences with those exposed for 1 month.

The thin-layer samples used for AFM investigations were prepared in two steps: (i) Films of various thicknesses in the range from 70 to 250 nm were spin-coated onto methanol washed glass slides at 500−4000 rpm from chloroform solutions of different concentrations. These films were melted again at 250 °C for 10 min and quenched at 0 °C within ice−water. (ii) After removing water under vacuum, these films were exposed at different temperatures for different times. After exposure the excess solvent was soaked out with lint-free tissue, and the films were dried in air at room temperature. Films were also spin-coated on silicon wafers under the same conditions, and the single wavelength ellipsometry technique was used to determine their thickness (PLASMOS SD2300 ellipsometer).

Differential Scanning Calorimetry. DSC thermograms of the solvent-induced bulk samples were recorded by means of a Perkin-Elmer DSC 7. The samples were introduced into stainless steel sample pans that were hermetically sealed from the atmosphere. Weight loss was checked after each experiment. Heating rates of 5 and 10 °C/min were used. It is worth emphasizing that for each run a new sample was used on account of the irreversibility of the solvent-induced crystal-

[†] Permanent address: Département de Physique, Faculté des Sciences et Techniques du Guéliz Université Cadi-Ayyad, B.P 549, MA-40000 Marrakech, Morocco.

[‡] Present address: Division of Molecular Material Science, Graduate School of Science, Osaka City University, 3-3-138, Sugimoto, Sumiyoshi-ku, Osaka 558-8585, Japan.

* Corresponding author: e-mail guenet@ics.u-strasbg.fr; tel +33 (0) 388 41 40 00; fax +33 (0) 388 41 40 99.

10.1021/ma049701x CCC: $27.50
Published on Web 05/08/2004

lization process. Irreversibility is taken here in the sense that after melting and cooling the second heating run does no longer correspond to a solvent-induced crystallization but to a crystallization from a highly concentrated solution instead. Because of this "one-run" procedure, together with the use of stainless steel pans, random noise cannot be avoided. This sometimes results in the appearance of sharp peaks foreign to the actual thermal behavior.

Polymer concentrations were determined by weighing the samples after drying for several hours under vacuum at 50 °C. For each systems, five samples were used in order to assess the experimental scatter. The concentrations given in what follows are bracketed between the lowest and the highest values found for the system under consideration.

Atomic Force Microscopy. AFM experiments were carried out on the dried films at room temperature in air using a Nanoscope III instruments (Digital Instruments, Santa Barbara, CA). Most of the images were obtained by means of the tapping mode (height and phase) with a silicon nitride cantilever (Olympus Optical Co. Ltd., Japan) of spring constant 42 N/m and of resonating frequency 300 kHz. The scanning rates were varied from 1 to 2 Hz. All images presented in this work were obtained reproducibly over at least three spots on the sample surfaces.

X-ray Diffraction. X-ray diffraction patterns were obtained on a Philips PW1009 instrument equipped with a Luzzati-Baro camera. Cu Kα radiation with a wavelength of 0.154 nm was used. The intensity was recorded by means of a linear detector coupled to a computer for data processing. All the experiments were carried out at room temperature.

Results and Discussion

In the case of solution-cast samples of isotactic polystyrene the alteration of a few degrees of the preparation temperature at constant polymer concentration produces totally different molecular structures and morphologies. As reported in ref 11, three different types of phases differing from the usual nonsolvated crystalline phase, namely the gel phase, the s-phase, and the p-phase, can be grown from iPS/*cis*-decalin solutions within a range of 20 °C. Typically, one observes the gel phase when annealing below 20 °C, the so-called s-phase between 20 and 30 °C, the so-called p-phase between 33 and 55 °C, and finally the usual crystalline phase above 55 °C. The first three phases consist of polymer−solvent compounds. Conversely, only two phases can grow from iPS/*trans*-decalin solutions: the gel phase when the preparation temperature stands below 20 °C, which also consists of a polymer−solvent compound, and the nonsolvated crystalline phase when annealing above 20 °C. Note that the effect of molecular weight, and correspondingly of polydispersity, has been shown to play no detectable role in the formation of the iPS/solvent compounds.[10]

As will be shown below, the same behavior as far as phases are concerned occurs with solvent-exposed samples. It is worth emphasizing that for solvent-exposed samples iPS differs notably from syndiotactic polystyrene (sPS). For iPS a change of exposure temperature within a limited range (4−40 °C) may reveal as many as four different phases, whereas with sPS the exposure temperature can be varied in a large range without drastically changing the nature of the coexisting phases. For instance, in sPS/toluene systems variation from 20 to 75 °C only changes the proportion of phases but not their nature.

Exposure Temperature T_{expo} = 4 °C. DSC traces obtained for iPS samples exposed to *cis*-decalin and *trans*-decalin can be seen in Figure 1. In *cis*-decalin two different events are observed. At T = 40 °C a melting

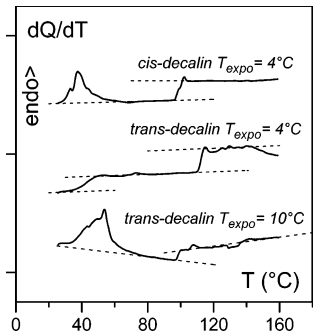

Figure 1. DSC traces for solid iPS samples exposed to decalin (either *cis* or *trans* as indicated) at 4 °C and also at T_{expo} = 10 °C for *trans*-decalin. Heating rate 10 °C/min.

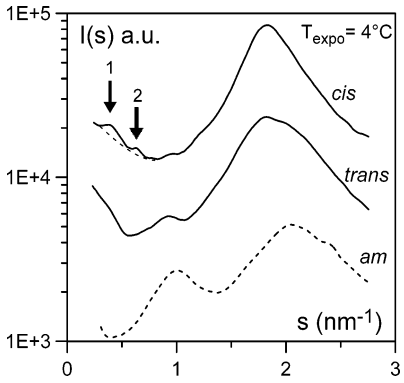

Figure 2. Diffraction patterns for solid iPS samples exposed to decalin (either *cis* or *trans* as indicated) at 4 °C and for amorphous isotactic polystyrene (dashed line). Reflections for iPS/*cis*-decalin systems are indicated (**1** for $s = 0.52$ nm^{-1} and **2** for $s = 0.84$ nm^{-1} with $s = 2/\lambda \sin \theta/2$).

Table 1. Polymer Concentration (w/w) Reached after Exposure to Liquid Solvent at T_{expo}

T_{expo} (°C)	iPS/*cis*-decalin	iPS/*trans*-decalin
4	0.36	0.39
10	0.36	0.39
25	0.3	0.32
30	0.32	0.39
40	0.13	0.18

event occurs while at T = 92 °C a second-order transition takes place (heat capacity jump). The latter most certainly corresponds to a glass transition process. In *trans*-decalin two events are also seen, yet they are both of second order (C_p jump). Both solvents do not therefore produce the same state, an outcome which was already reported in the case of solution-cast samples.[11] It is worth noting that the temperature associated with the melting event observed here corresponds within experimental uncertainties to that reported for similar systems obtained from solution-cast samples.[11]

The polymer concentration are rather high: in *cis*-decalin $C_{pol} = 0.36 \pm 0.03$ (w/w), and in *trans*-decalin $C_{pol} = 0.39 \pm 0.03$ (w/w). (These values are reported in Table 1.) These are global values since, as will be discussed below, two-phase systems are dealt with.

The X-ray diffraction pattern recorded for iPS/*cis*-decalin systems supports the existence of two phases, one of which corresponds to the polymer−solvent compound and another to the amorphous phase (see Figure 2). Two diffraction maxima are indeed observed at $s = 0.52$ nm^{-1} and $s = 0.84$ nm^{-1} which stand for the stem spacing ($d \approx 2$ nm) as already reported for this iPS/*cis*-decalin compound.[11] A broad halo is seen at larger

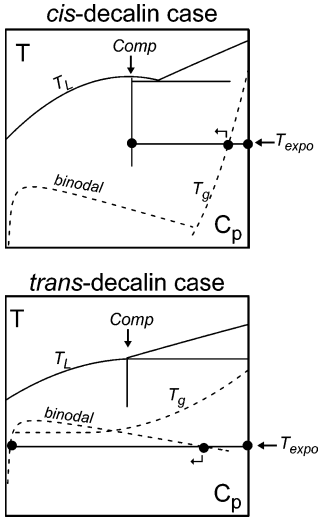

Figure 3. Hypothetical temperature−concentration phase diagrams for *cis*-decalin (upper diagram) and *trans*-decalin (lower diagram). "Comp" indicates the stoichiometric composition of the compound. T_L is the liquidus line, T_g the glass transition line, and T_{expo} the exposure temperature.

angles ($s \approx 1.8$ nm^{-1}) arising from the superimposition of the diffraction pattern of amorphous iPS and of the solvent halo. Conversely, the diffraction pattern typical of amorphous systems is seen for samples exposed to *trans*-decalin.

These results can be explained if one takes into account two major aspects of these solvents toward isotactic polystyrene: (i) the propensity of these two solvents to form polymer−solvent compounds with this polymer;[10−15] (ii) the existence of a miscibility gap yet with differing theta temperatures ($\theta = 18$ °C in *trans*-decalin and $\theta = 12$ °C in *cis*-decalin).[19] Note also that, as was emphasized by Klein and Guenet,[20] these two solvents possess differing melting enthalpies, which further highlights their differing interactions ($\Delta H_m = 61.3$ J/g for *cis*-decalin against $\Delta H_m = 95$ J/g for *trans*-decalin). The use of the hypothetical phase diagrams drawn in Figure 3 can help throw some light on the thermal behavior shown in Figure 1. In *trans*-decalin one may assume that for $T_{expo} = 4$ °C the whole system stands always under its T_g (glass transition), especially so as the T_g line (variation of T_g with concentration) becomes temperature-nonvariant within the miscibility gap. As a result, when the polymer concentration is such that the system enters the miscibility gap, two phases are formed: a polymer-rich and a polymer-poor phase. As is portrayed in Figure 3, these two phases are likely to undergo glass transition at two different temperatures, as is observed from DSC traces. Note that, although T_g is a second-order transition, the T_g line obeys Gibbs phase rule and therefore must remain at constant temperature within the miscibility gap.[21]

Conversely, in *cis*-decalin, as the miscibility gap is located at temperatures lower than in *trans*-decalin since $\theta_{cis} < \theta_{trans}$, one may surmise that the T_g line meets the miscibility gap at much lower temperatures than in *trans*-decalin. As a result, while one phase will still be highly concentrated, and thus undergo a glass transition process on heating, we may contemplate the case where the second phase be less concentrated and defined by *T,C* coordinates such as to stand above the T_g line. Under these conditions this phase can form a polymer−solvent compound. The resulting DSC traces

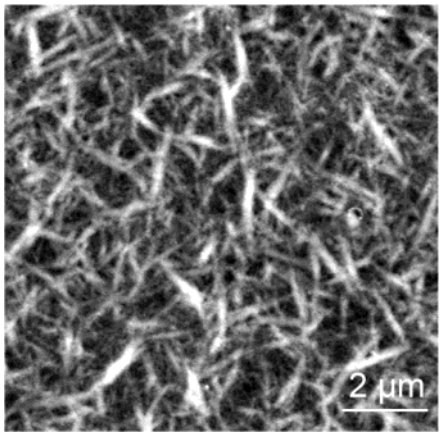

Figure 4. AFM picture of the morphology of iPS/*cis*-decalin systems formed after exposure of solid iPS samples at 4 °C.

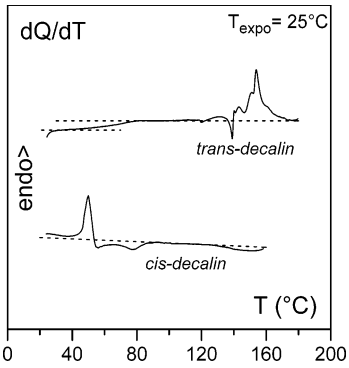

Figure 5. DSC traces for solid iPS samples exposed to decalin (either *cis* or *trans* as indicated) at 25 °C. Note that the apparent exotherm near $T = 145$ °C is actually a random noise. Heating rate 10 °C/min.

should therefore exhibit a melting event corresponding to the melting of the polymer−solvent compound and a C_p jump related to the glass transition of the highly concentrated phase. The use of these hypothetical phase diagrams is further consistent with the results obtained at $T_{expo} = 10$ °C for iPS/*trans*-decalin systems. As a matter of fact, the behavior is now similar to that observed for iPS/*cis*-decalin systems, namely an endotherm corresponding to the occurrence of a compound and a T_g event (Figure 1). Note that the iPS/*trans*-decalin endotherm stands at a higher temperature than the iPS/*cis*-decalin endotherm, which is in agreement with previous results[3] and is related to the lower degree of solvation of the compound formed in this system.

Interestingly, the morphology of iPS/*cis*-decalin systems exposed at $T_{expo} = 4$ °C as observed by AFM (Figure 4) reveals a fibrillar structure, similar to that reported for solution-cast samples for which fibrillar thermoreversible gels are produced.[3] Some domains seem to be larger than the average fibril size (white domains on Figure 4) and may stand for the polymer concentrated phase that undergoes the glass transition on heating. Conversely, no noticeable features have been observed with *trans*-decalin.

Exposure Temperature $T_{expo} = 25$ °C. Here, both systems stand well above the miscibility gap. Therefore, no liquid−liquid phase separation is involved. Typical DSC traces are shown in Figure 5, where a melting event can be observed with both solvents yet at significantly differing temperatures: $T_m \approx 50$ °C in *cis*-decalin and $T_m \approx 150$ °C in *trans*-decalin. In both solvents the concentrations are rather high: $C_{pol} = 0.33 \pm 0.03$

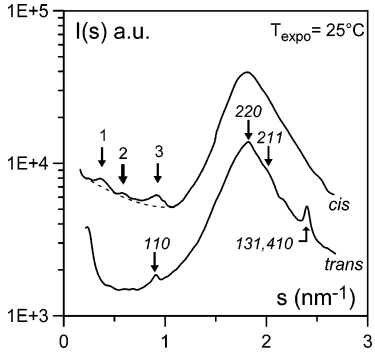

Figure 6. Diffraction patterns for solid iPS samples exposed to decalin (either *cis* or *trans* as indicated) at 25 °C. Reflections observed for iPS/*cis*-decalin systems are indicated (**1** for $s = 0.39$ nm^{-1}, **2** for $s = 0.59$ nm^{-1}, and **3** for $s = 0.909$ nm^{-1} with $s = 2/\lambda \sin \theta/2$). Positions of the reflections of the main crystallographic planes of Natta's lattice are also indicated by arrows.

(w/w) in *cis*-decalin and $C_{pol} = 0.36 \pm 0.03$ (w/w) in *trans*-decalin. Note that in *trans*-decalin there might be the occurrence of a glass transition at $T_g \approx 70$ °C which might arise from parts of the sample not fully swollen.

These results are similar to those obtained from solution-cast samples. In *trans*-decalin prominent diffraction maxima are observed at $s = 0.926$ nm^{-1} and $s = 2.39$ nm^{-1} as well as others, somewhat weaker because of being obliterated by the solvent halo, at $s = 1.81$ nm^{-1} and $s = 2.03$ nm^{-1} (Figure 6). These prominent maxima are consistent with the presence of classical nonsolvated crystals as they correspond to the 110 and 131, (410) crystallographic planes of the lattice derived by Natta[22] (designated in what follows as Natta's lattice). Clearly, no polymer−solvent compound is formed as was also reported for solution-cast iPS/*trans*-decalin at this temperature.[11]

Conversely, in *cis*-decalin there is again the formation of a polymer−solvent compound. These conclusions are confirmed by X-ray diffraction data reported in Figure 6 where diffraction maxima are seen for $s = 0.39$ nm^{-1}, $s = 0.59$ nm^{-1}, and $s = 0.909$ nm^{-1}. They correspond to those values reported for the so-called s-phase which has been described earlier by Guenet et al.[11] Note that the third maximum ($s = 0.909$ nm^{-1}) does not stand here for the 110 plane of nonsolvated crystals but to the 11 plane of a two-dimensional lattice proposed for the s-phase.[11] (There is no correlation along the *c*-axis, namely, parallel to the helical structure of the polymer.) The absence of a reflection at $s = 2.39$ nm^{-1}, as would give the 131 plane of Natta's lattice, allows one to support this point (refer to the above case of *trans*-decalin). The s-phase is known to display higher molecular order than the gel phase[11] and is made up of an assembly of spherulites as opposed to an array of fibrils. Figure 7 shows the AFM image of the spherolites obtained here in *cis*-decalin by solvent exposure, quite similar to those observed from solution-cast systems.

Exposure Temperature $T_{expo} = 30$ °C. The results are similar to those obtained at $T_{expo} = 25$ °C. Typical DSC traces are presented in Figure 8. Melting endotherms are observed with both solvents, yet again at significantly differing temperatures: $T_m \approx 50$ °C in *cis*-decalin and $T_m \approx 150$ °C in *trans*-decalin. In both solvents the concentration are rather high: $C_{pol} = 0.32 \pm 0.03$ (w/w) in *cis*-decalin and $C_{pol} = 0.39 \pm 0.03$ (w/w) in *trans*-decalin. Similar conclusions as those drawn for $T_{expo} = 25$ °C also hold here.

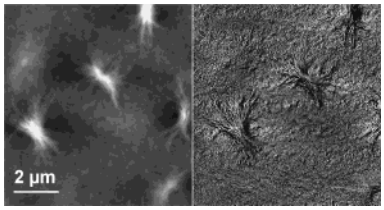

Figure 7. AFM picture of the morphology of iPS/*cis*-decalin systems formed after exposure of solid iPS samples at 25 °C: left, normal mode; right, tapping mode.

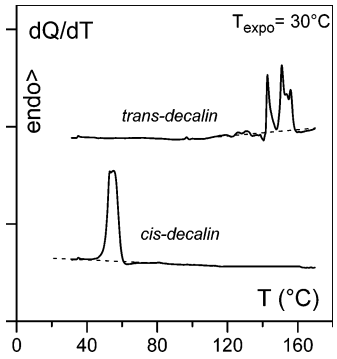

Figure 8. DSC traces for solid iPS samples exposed to decalin (either *cis* or *trans* as indicated) at 30 °C. Heating rate 10 °C/min.

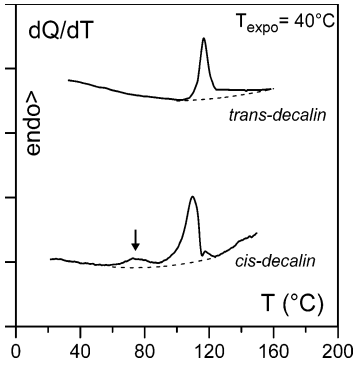

Figure 9. DSC traces for solid iPS samples exposed to decalin (either *cis* or *trans* as indicated) at 40 °C. Heating rate 10 °C/min. Arrow indicates the peritectic melting.

Exposure Temperature $T_{expo} = 40$ °C. As shown in Figure 9, there is a significant change in the DSC traces of systems prepared from exposure to *cis*-decalin. A small melting endotherm is seen at about $T = 75$ °C immediately followed by a larger one at $T = 110$ °C. In iPS/*trans*-decalin systems only one endotherm is seen at $T = 110$ °C. The DSC traces in iPS/*cis*-decalin systems are quite similar to those obtained from solution-cast samples, for which this thermal behavior has been interpreted by considering the existence of another phase, the p-phase, which is also a solvated phase. Under these conditions, the first endotherm corresponds to the desolvation process (see comment below), namely, a peritectic or incongruently melting, while the second endotherm stands for the melting of the nonsolvated crystals. This is the reason why the second melting endotherm occurs at a temperature close to that observed in iPS/*trans*-decalin systems, where only nonsolvated crystals form at this exposure temperature. Interestingly, in both systems the polymer concentration is significantly lower than that reached with the previously considered exposure temperatures ($C_{pol} = 0.13 \pm 0.03$ (w/w) in *cis*-decalin and $C_{po} = 0.1\,8 \pm 0.03$ (w/w) in *trans*-decalin). Note that the first event at 75 °C

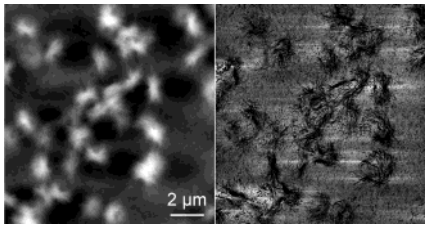

Figure 10. AFM picture of the morphology of iPS/*cis*-decalin systems formed after exposure of solid iPS samples at 40 °C: left, normal mode; right, tapping mode.

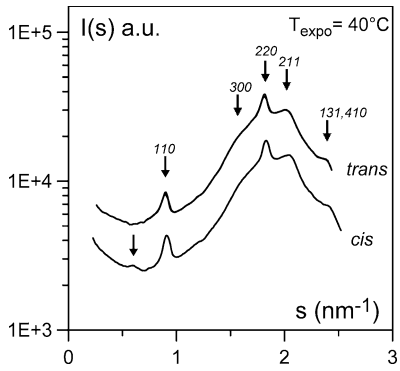

Figure 11. Diffraction patterns for solid iPS samples exposed to decalin (either *cis* or *trans* as indicated) at 40 °C. Arrow indicates the additional reflection observed for iPS/*cis*-decalin systems with respect to Natta's lattice (for $s = 0.59$ nm^{-1} with $s = 2/\lambda \sin \theta/2$). Positions of the reflections of the main crystallographic planes of Natta's lattice are also indicated by arrows.

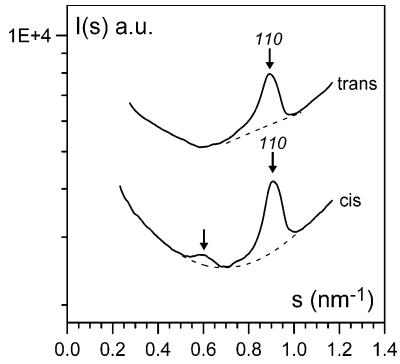

Figure 12. Diffraction patterns for solid iPS samples exposed to decalin at 40 °C highlighting the additional reflection ($s = 0.59$ nm^{-1}) observed for iPS/*cis*-decalin systems with respect to the 110 plane of Natta's lattice.

cannot be taken as a glass transition event under this concentration condition.

Note that the p-phase also possesses a spherolitic morphology as observed from AFM investigations (Figure 10).

The X-ray diffraction observed with these samples (Figure 11) shows in both solvents reflections arising from the usual nonsolvated crystals (Natta's lattice), yet in the case of *cis*-decalin an additional reflection is observed at $s = 0.59$ nm^{-1} (Figure 12), namely $d \approx 1.7$ nm, a distance which is about the value of the 100 plane of Natta's lattice ($d_{100} = 1.82$ nm). Keeping in mind that a peritectic is formed, we suspect that this reflection arises from solvent intercalation in the cavities of Natta's lattice as is highlighted in Figure 13. On this basis, we can tentatively account for this reflection by contemplating a simple argument. Normally, the 100 reflection is forbidden because Natta's lattice contains

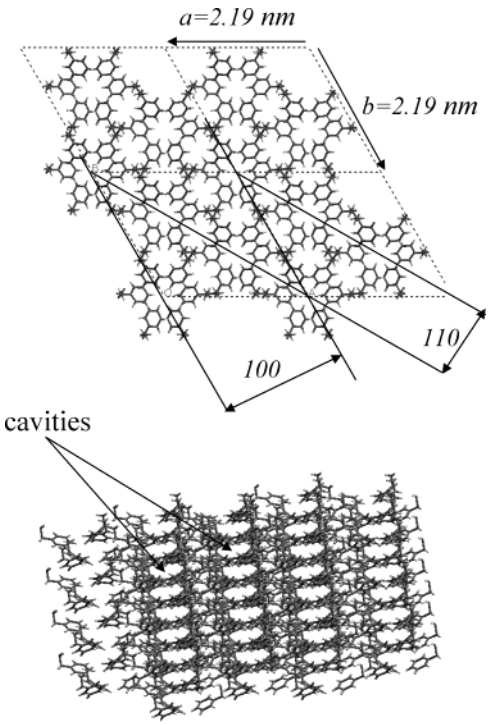

Figure 13. Sketch of the crystal organization of the Natta's lattice (space group *R*3*c*) drawn by using the Cerius 42 software from Accelerys. The helical structure is a 3_1 helix. Upper: four adjacent lattices as seen parallel to the helix axis. Lower: assembly of 12 lattices as seen nearly perpendicular both to the helix axis and to the 210 plane. Arrows indicate the possible cavities. The present representation does not use van der Waals radii, so that the cavities are actually smaller but still of sufficient volume to house *cis*-decalin molecules.

two rows of polymer stems between consecutive 100 planes which entails destructive interferences. If *cis*-decalin molecules are housed within some of the cavities shown in Figure 13, then additional rows of diffracting material are present between consecutive 100 planes, which are liable to give rise to constructive interferences and hence the appearance of a 100 reflection.

Concluding Remarks

The results presented herein highlight that the structure and the thermodynamic behavior of iPS/decalin systems, namely the nature of the phases that are formed, do not depend on the path followed to produce them. Whether concentration is decreased to C_0 at constant temperature T_0 (solvent-exposed) or temperature is rapidly lowered to T_0 at constant concentration C_0 (solution-cast) does not make any significant difference: the same phases are produced.

These outcomes give further support to recent conclusions drawn from the study of sPS/solvant systems. They also emphasize that Gibbs phase rules can be used to establish $T-C$ phase diagrams with these systems since they behave like systems at equilibrium as has been discussed recently.[23]

Acknowledgment. Dr. Biswajit Ray is greatly indebted to the French Government (Ministère de la Recherche) for a postdoctoral grant in aid. The authors are indebted to Suzanne Zehnacker for carrying out the DSC experiments and to André Mathis for performing the X-ray diffraction experiments.

References and Notes

(1) Girolamo, M.; Keller, A.; Miyasaka, K.; Overbergh, N. *J. Polym. Sci., Polym. Phys.* **1976**, *14*, 39.
(2) Spěvaček, J.; Schneider, B. *Adv. Colloid Interface Sci.* **1987**, *27*, 81.
(3) Guenet, J.-M. *Thermoreversible Gelation of Polymers and Biopolymers;* Academic Press: London, 1992.
(4) Vittoria, V.; de Candia, F.; Ianelli, P.; Immirzi, A. *Makromol. Chem. Rapid Commun.* **1988**, *9*, 765.
(5) Vittoria, V.; Russo, R.; de Candia, F. *Makromol. Chem. Macromol. Symp.* **1990**, *39*, 317.
(6) Vittoria, V.; Russo, R.; de Candia, F. *Polymer* **1991**, *32*, 3371.
(7) Vittoria, V.; Ruvolo Filho, A.; de Candia, F. *Polym. Bull. (Berlin)* **1991**, *26*, 445.
(8) Ray, B.; El Hasri, S.; Thierry, A.; Marie, P.; Guenet, J. M. *Macromolecules* **2002**, *35*, 9730.
(9) El Hasri, S.; Thierry, A.; Schweyer, F.; Guenet, J. M. *Macromol. Symp.* **2001**, *166*, 123.
(10) Guenet, J. M.; McKenna, G. B. *Macromolecules* **1988**, *21*, 1752.
(11) Guenet, J. M.; Menelle, A.; Schaffhauser, V.; Terech, P.; Thierry, A. *Colloid Polym. Sci.* **1994**, *272*, 36.
(12) Itagaki, H.; Takahashi, I. *Macromolecules* **1995**, *28*, 5477.
(13) Itagaki, H. *Macromol. Symp.* **2001**, *166*, 13.
(14) Nakaoki, T.; Kobayashi, M. *J. Mol. Struct.* **1991**, *242*, 315.
(15) Nakaoki, T.; Katagiri, C.; Kobayashi, M. *Macromolecules* **2002**, *35*, 7708.
(16) Natta, G. *J. Polym. Sci.* **1955**, *16*, 143.
(17) Benoit, H.; Grubisic, Z.; Rempp, P.; Decker, D.; Zilliox, J. G. *J. Chim. Phys.* **1966**, *63*, 1507.
(18) Guenet, J. M.; Gallot, Z.; Picot, C.; Benoit, H. *J. Appl. Polym. Sci.* **1977**, *21*, 2181.
(19) Berry, G. C. *J. Chem. Phys.* **1966**, *44*, 4450.
(20) Klein, M.; Guenet, J. M. *Macromolecules* **1989**, *22*, 3716.
(21) Zarzycki, J. *Faraday Discuss. Chem. Soc.* **1971**, *50*, 122.
(22) Natta, G.; Corradini, P.; Bassi, I. W. *Nuov. Cim. Suppl.* **1960**, *15*, 68.
(23) Guenet, J. M. *Macromol. Symp.* **2003**, *203*, 1.

MA049701X